Simulation of Seismic Collapse in Nonductile Reinforced Concrete Frame Buildings with Masonry Infills

Henry Burton, S.E.[1]; and Gregory Deierlein, F.ASCE[2]

Abstract: Improved analysis methods and guidelines are presented to simulate the seismic collapse of nonductile concrete frame buildings with masonry infills. The analysis tools include an inelastic dual-strut model that captures the post-peak behavior of the masonry infill and its interaction with the surrounding frame. The dual compression struts capture the column-infill interaction that can cause shear failure of the columns and loss of their vertical load carrying capacity. A rigid softening shear degradation model is implemented in the beam-column elements to capture the shear failure of nonductile RC columns. Guidelines are presented to determine the strut model parameters based on data from 14 experimental tests on infill frames. The models are applied in three-dimensional nonlinear dynamic analyses of a three-story nonductile concrete frame prototype building with infills. The incremental dynamic analyses technique is utilized to understand the effect of the infill-column interaction and the rocking of shallow foundations on collapse performance, including a parameter study to examine the sensitivity of the results to the assumed strength and deformation parameters of the infill walls. Collapse assessment of the prototype building indicates that incorporating infill strut-column interaction and the shear degradation of columns is critical to the prediction of the collapse capacity of nonductile infill frames. Otherwise, the omission of this deterioration mechanism leads to unconservative collapse capacity predictions. The analyses further demonstrate that rocking of shallow foundations has a favorable effect on the collapse performance of infill frames and that the infill strut strength has considerably greater influence on collapse performance than the infill strut deformation parameters. **DOI: 10.1061/(ASCE)ST.1943-541X.0000921.**

Author keywords: Infills; Rocking; Concrete; Collapse; Earthquake engineering; Seismic effects; Modeling; Analysis and computation.

Introduction

Concrete frame buildings with infills are commonly used throughout the world, both in developing and industrialized countries. Experience with past earthquakes has shown that frames with infills, particularly those with nonductile concrete frames, are prone to collapse under earthquakes. In densely populated urban centers around the world, the prevalence of nonductile infill frame buildings presents a significant seismic risk. Effective mitigation of this risk requires reliable methods to assess the collapse behavior of these buildings.

This study develops improved analysis tools and guidelines to simulate the seismic collapse of nonductile concrete frame buildings with masonry infills, incorporating important mechanisms related to frame-infill interaction and foundation rocking, which have not been previously addressed. Sattar and Liel (2010) assessed the collapse performance of infill frames, simulating the infills with inelastic compression-only struts to represent the diagonal compression behavior of the infill. However, this modeling approach does not fully capture the interaction between the infill and the surrounding frame, particularly the force transfer that can lead to column shear failure near the beam-column joints. In extreme cases, the column shear failure can lead to loss in the axial (gravity) load carrying capacity of the columns. To overcome this limitation, in this paper, a pair of compression-only struts is employed in each loading direction to simulate the local force transfer between the column and the infill. Another question that has not been previously addressed is the effect of uplifting (rocking) of shallow column foundations on seismic response. Rocking of shallow foundations is known to have both positive and negative effects on seismic performance. On one hand, column footing uplift can serve as a fuse-like mechanism that tends to reduce seismic force demands on the superstructure. However, rocking can also increase the axial loads on columns, which may lead to compression failures in the column and/or foundation. This increase in axial demands results from the additional gravity load that must be carried by the compression-side column in a rocking frame. In this study, compression-only elements are used at the bases of columns to capture this uplift behavior.

Many researchers have developed analytical equations to determine the strength and stiffness parameters of infill strut models. The following provides an overview of four models that are frequently cited in the literature.

1. ASCE/Structural Engineering Institute (SEI) Standard 41 (2007), Section 7.4.2, provides guidelines for calculating the width of an equivalent strut to represent a solid infill panel prior to cracking. This equivalent strut width is determined by using the relative stiffness of the infill and the surrounding frame and is based on pioneering work by Stafford-Smith and Carter (1969). The compressive (crushing failure) strength of the strut is calculated based on this equivalent width, the infill thickness, and the prism compressive strength of the infill. ASCE/SEI 41 also provides an equation for calculating the in-plane sliding shear strength of the panel, which can likewise be transformed into an equivalent strut strength, and the limiting value between the two strut strengths is used. A secant

[1]Ph.D. Candidate, Dept. of Civil Engineering, Stanford Univ., Blume Center, 439 Panama Mall, Building 540, Room 118, Stanford, CA 94305 (corresponding author). E-mail: hburton@stanford.edu

[2]Professor, Dept. of Civil Engineering, Stanford Univ., Blume Center, 439 Panama Mall, Building 540, Room 118, Stanford, CA 94305.

Note. This manuscript was submitted on December 29, 2012; approved on July 31, 2013; published online on August 3, 2013. Discussion period open until September 18, 2014; separate discussions must be submitted for individual papers. This paper is part of the ***Journal of Structural Engineering***, © ASCE, ISSN 0733-9445/A4014016(10)/$25.00.

stiffness, measured to the compressive strength of the strut, is computed based on the geometry of the strut and the prism modulus of the infill, and the initial stiffness of the strut is recommended to be twice the secant stiffness.

2. Dolsek and Fajfar (2008) proposed equations for calculating the initial stiffness and maximum strength of an equivalent infill strut. The maximum strength equation is based on the cross-sectional area of the panel, the aspect ratio, and the prism cracking strength of the infill. The initial stiffness is the shear stiffness of the infill panel transformed in the direction of the equivalent strut.
3. Saneinejad and Hobbs (1995) proposed equations for calculating the ultimate strength and initial stiffness of an infill compressive strut. The equivalent strut strength is based on four failure mechanisms: corner crushing, which is crushing of the infill in at least one of the loaded corners, diagonal compression mode which is crushing within the central region, shear mode which is horizontal shear failure through the bed joints of the masonry infill and diagonal cracking. The corresponding lateral deflection at peak load is computed based on an equivalent strut strain corresponding to the infill strain at the peak uniaxial compression from prism tests. This lateral deflection is used to compute the secant stiffness at the peak load, with the initial stiffness taken as twice this secant stiffness.
4. Mehrabi et al. (1996) proposed a limit state analytical method for calculating the lateral strength of infill frames. This method involves strength evaluations for the following five possible failure mechanisms: (1) horizontal shear failure of infill and flexural hinging of columns, (2) lateral infill sliding combined with diagonal cracking and shear/flexural failure of columns, (3) infill crushing and column flexural hinging near beam-column joints, (4) infill crushing and flexural hinging at top and bottom of column, and (5) lateral sliding of infill and flexural hinging of columns.

In this study, these methods are tested against data from 14 experiments and the results are used to develop guidelines to determine equivalent infill strut parameters that are critical to collapse assessment. The most influential strut model parameters are identified based on the results of a systematic parametric study.

Previous studies on seismic collapse assessment of concrete buildings have typically been performed using two-dimensional (planar) analysis models, ignoring the lateral resistance provided by gravity framing and sharing of seismic forces through the floor diaphragm. In this study, collapse simulation is performed using three-dimensional non-linear analysis models that include gravity framing elements and rigid floor diaphragm constraints.

Infill Strut Model Development

Characterizing the nonlinear behavior of infills is critical to the simulation of collapse in infill frames, particularly the postpeak behavior. Fig. 1 illustrates how the infill panels are simulated using two opposing pairs of diagonal compression-only struts with inelastic degrading response incorporated using a peak-oriented hysteretic model that is described later. In each direction, a diagonal strut is placed between the nodes representing the beam–column joints, and an off-diagonal strut is used to capture the interaction between the infill and the columns. Chrysostomou (1991) used the principle of virtual displacements to investigate the force and stiffness distribution between central and off-diagonal struts for infill frames. Chrysostomou found that (1) the force and stiffness distribution is a function of the lateral displacement of the wall and

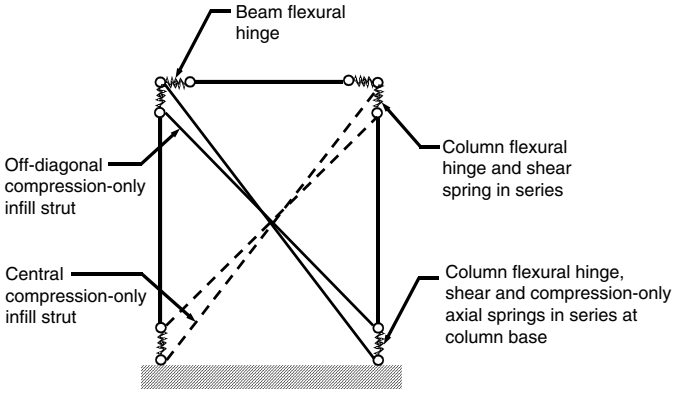

Fig. 1. Schematic of typical infill frame model

(2) the maximum force delivered to the off-diagonal strut is approximately 25% of the total strut force. For this study, 25% of the total strut stiffness is assigned to the off-diagonal strut and 75% to the central strut. Fig. 2 shows the general trilinear monotonic backbone curve for the inelastic strut model. The force-deformation relationship for the central and off-diagonal struts is shown in Fig. 3.

The peak oriented hysteretic model described by Ibarra et al. (2005) is adapted and used to capture the nonlinear behavior of the infill compression struts. The model was originally implemented for beam-column plastic hinges in *OpenSees* by Lignos and Krawinkler (2013) and is adapted for axial response of infill struts in this study. The hysteretic strut model requires the specification of five parameters to control the monotonic and cyclic behavior: the yield strength (F_y), the initial stiffness (K_e), the capping or ultimate strength (F_c), the plastic capping displacement (Δ_{cap}^{p}), and either the postcapping displacement (Δ_{pc}) or degrading postcapping stiffness (K_c).

The strut model parameters are obtained through calibration to available experimental data for infill portal frame specimens whose designs matched the prototype building used in this study. However, with the goal toward developing general recommendations for infill strut parameters, this study also evaluates previously proposed analytical models for predicting strength and stiffness. Lateral strength and stiffness predictions for the 14 test specimens

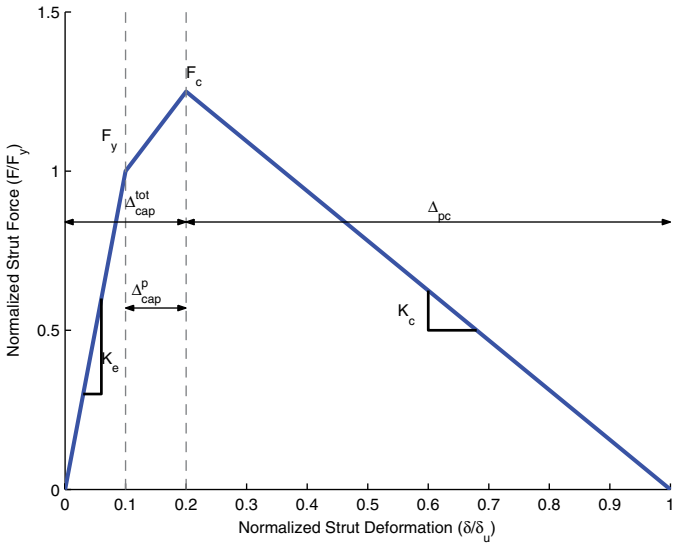

Fig. 2. Trilinear backbone curve for infill strut model

J. Struct. Eng., 2014, 140(8): A4014016

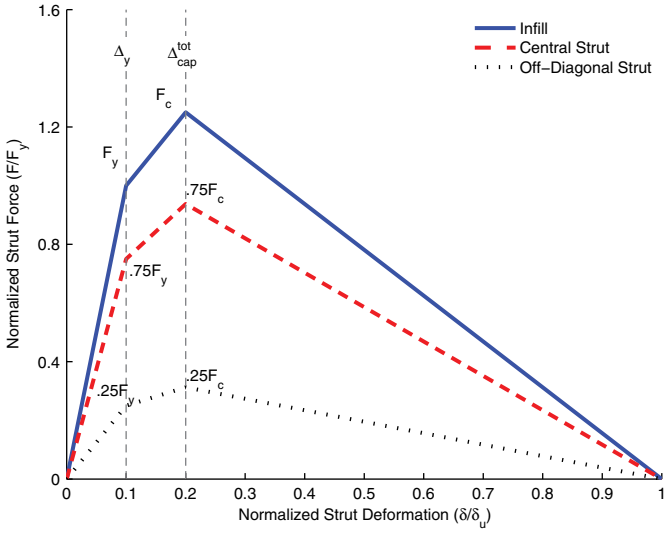

Fig. 3. Force-deformation relationships for central and off-diagonal struts relative to infill

were obtained from analytical models proposed by ASCE/SEI 41 (2007), Dolsek and Fajfar (2008), and Saneinejad and Hobbs (1995). Mehrabi et al. (1996) only developed models to predict lateral strength. The models were tested against data from 14 single story, single bay test specimens with solid infill panels, taken from four different experimental programs.

Table 1 shows a comparison of the ratio of predicted strut ultimate strength and initial stiffness from each of the models to the measured values. The limit state approach used by Mehrabi et al. (1996), which incorporates five failure mechanisms, provides the best estimate of lateral strength based on the root mean square (RMS) of the normalized errors. As shown in the table, the ratio of calculated to measured strength ranges from 0.53 to 2.11 for this model. On the other hand, the model by Dolsek and Fajfar (2008), which is based on a single failure mechanism, gives the least accurate prediction, in which the calculated to measured strengths range from 0.66 to 5.05. In general, the models with fewer numerical errors also better identify the observed failure mechanism. Predictions were significantly better for specimens that experienced infill panel failure mechanisms than for those that experienced beam and column failures. Although all of the models generally overestimated the strength of specimens that experienced failures in framing members, this discrepancy is not a major concern for this study, in which the strength and stiffness deterioration of the beam-column elements are explicitly modeled in the nonlinear analyses. The initial lateral stiffness obtained from the test data is defined as the slope of a line connecting the origin to the point on the cyclic skeleton curve at a load equal to 50% of the maximum lateral resistance. Overall, the model by Saneinejad and Hobbs (1995) provides the best estimate of lateral stiffness for the test specimens based on the minimum RMS of the normalized errors. The following additional observations are presented as guidelines for the use of the model parameters:

- The ratio of the peak (capping) strength of the infill to the yield strength (F_c/F_y) ranged from 1.2 to 1.6 for the 14 tests with a mean of 1.4 and a coefficient of variation of 0.09;
- The ratio of capping drift of the infill to yield drift (Δ_c/Δ_y) ranged from 2.6 to 6.5 for the 14 tests, with a mean ratio of 4.5 and a coefficient of variation of 0.24; and
- There was a strong correlation between the failure mechanism at peak load and the ratio of post-peak to initial stiffness (K_c/K_e). Test specimens that experienced beam-column failure mechanisms at peak loads have a mean ratio of the post capping degrading stiffness to the initial stiffness of 0.067. Test specimens that experienced infill panel failure mechanisms at peak loading have a mean ratio of post capping to initial stiffness of 0.035. Thus, this 0.035 ratio of postcapping stiffness to initial stiffness is suggested when beam-column failure mechanisms are explicitly considered in the collapse assessment models, as is the case in this study. Consideration of this postpeak softening behavior is recommended for consideration as an improvement to the elastic-plastic infill wall strut model that is currently used in the ASCE/SEI 41 (2007) standard for seismic rehabilitation.

Table 1. Comparing Infill Frame Properties from Model Predictions to Those Obtained from Test Results

Specimen number	Testing program/ specimen[a]	Ratio of predicted to measured lateral strength				Ratio of predicted to measured lateral stiffness			Failure mechanism for test specimen
		ASCE 41 (2007)	Dolsek and Fajfar (2008)	Saneinejad and Hobbs (1995)	Mehrabi et al. (1996)	ASCE 41 (2007)	Dolsek and Fajfar (2008)	Saneinejad and Hobbs (1995)	
1	K-SU1	0.67	2.33	0.99	0.88	0.88	4.58	0.26	Bed joint sliding
2	B-CU1	0.40	3.19	1.01	0.53	0.60	2.75	0.27	Diagonal cracking
3	M-S4	1.45	2.14	1.41	1.33	0.78	3.14	0.61	Diagonal cracking and sliding
4	M-S5	1.11	1.32	1.55	0.95	0.95	4.07	0.70	Diagonal cracking and sliding
5	M-S6	1.12	1.66	1.11	1.10	0.57	2.29	0.89	Diagonal cracking and sliding
6	M-S7	0.56	0.66	0.78	0.54	1.15	4.95	0.86	Diagonal cracking and sliding
7	M-S10	1.37	2.75	1.51	1.14	1.03	5.15	0.77	Diagonal cracking and sliding
8	M-S11	1.04	1.58	0.88	0.69	1.15	6.27	0.48	Diagonal cracking and sliding
9	C-C1	2.22	3.25	1.38	1.09	3.17	11.08	2.50	Beam/column flexural hinging
10	C-L1	2.15	4.40	1.83	1.87	3.22	13.69	2.63	Beam/column flexural hinging
11	C-N1	2.04	5.05	1.96	2.11	2.61	11.37	2.01	Beam/column flexural hinging
12	C-U1	3.20	4.67	2.35	1.78	4.77	16.62	2.20	Column shear failure
13	C-V11	1.96	4.85	1.93	1.23	4.03	17.68	1.90	Column shear failure
14	C-V21	1.56	3.86	1.22	0.70	3.01	13.26	2.10	Column shear failure
	RMS of normalized error	0.89	2.41	0.62	0.50	1.69	9.00	0.89	

[a]Specimen identification keys: *X-Y*, where *X* is the last initial of the author and *Y* is the specimen designation used in the experimental study; i.e., B = Blackard et al. (2009); C = Colangelo (2005); K = Kyriakides (2011); M = Mehrabi et al. (1996).

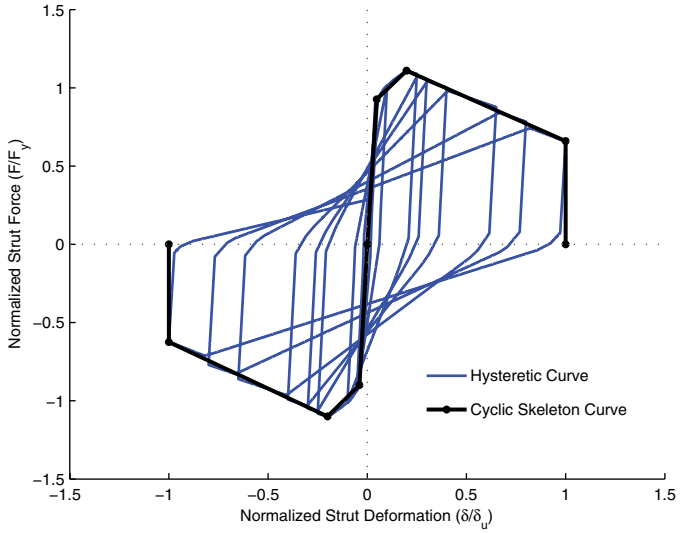

Fig. 4. Cyclic skeleton curve for infill strut model

The recommendations for strut model parameters described earlier are intended for infill frames with solid panels. Infill strut properties must be appropriately adjusted to account for the presence of openings. Several authors, including Giannakas et al. (1987), Asteris (2003), and Mondal and Jain (2008), have proposed reduction factors for the equivalent strut width based on the size and location of openings. The initial strength and stiffness strut model parameters can be adjusted by these recommendations.

Infill Strut Model Calibration

For the purposes of the collapse analyses described later, the hysteretic strut model was calibrated to a set of six 2/3 scale nonductile infill frames tested by Blackard et al. (2009). These consist of single story, single bay infill frames of different configurations that were subjected to quasi-static cyclic loading. The authors designed the specimens based on a prototype building model that is described later and used in the collapse safety assessment for this study. Three of the six test specimens (Specimens CU1, CU2, and CU5) encompass the specific infill frame configurations found in the prototype building: a solid infill panel, an infill panel with a window opening, and an infill panel with a door opening. Further details on the design of the specimens are presented in the work of Blackard et al. (2009). The current calibration was to obtain strut model parameters for the cyclic skeleton curve (Fig. 4) for these three conditions.

Calibration of the strut models was performed in *OpenSees*. Beams and columns were idealized using elastic elements with zero-length flexural plastic hinges and the masonry infill was modeled using two pairs of compression-only struts. The shear degradation model (discussed later) was included in the zero-length elements at the end of the columns. The parameters for the plastic hinges of the reinforced beams and concrete columns were obtained using the semi-empirical equations developed by Haselton et al. (2008). The properties of the compression struts were the subject of the current calibration effort, which entailed an iterative process whereby the experimental cyclic loading protocol was applied to the computational model and the strut model parameters were adjusted until there was a good visual match between the measured and simulated hysteretic curves. The parameters of primary interest include K_e, F_y, F_c/F_y, the ratio of capping displacement to yield displacement ($\Delta_{\text{cap}}^{\text{tot}}/\Delta_y$), and K_c/K_e or, alternatively, Δ_{pc}. Fig. 5 illustrates a comparison between the experimental results and the calibrated model prediction for two of the three specimens. The plots show good agreement between the calibrated model and experimental results, with the exception of the unloading stiffness, which is significantly steeper in the analysis model. This reflects a limitation in the current implementation of the hysteretic model in *OpenSees* that does not allow for degradation of unloading stiffness. The plots also show that the ratio of peak (capping) force to yield force is larger for the specimen with a window opening in the infill. The ratio of capping displacement to yield displacement and the absolute value of post-capping stiffness are also larger for the specimen with an opening in the infill.

Simulation of Column Shear Degradation

Nonductile concrete frames are generally prone to shear failure in beams and columns because of inadequate shear and confinement reinforcement. In infill frames, the interaction of the infill with the

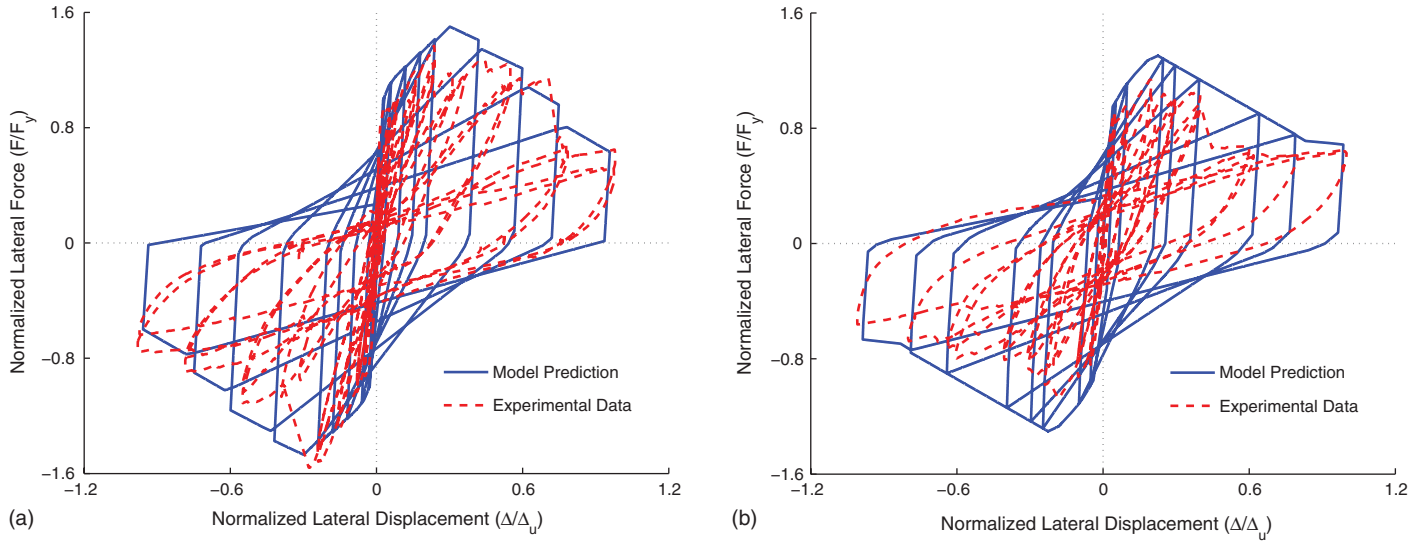

Fig. 5. Calibration of infill strut model to experimental test: (a) specimen with solid infill; (b) specimen with window opening in infill

J. Struct. Eng., 2014, 140(8): A4014016

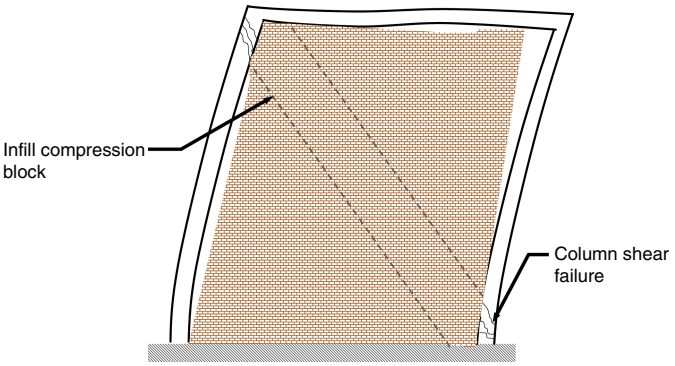

Fig. 6. Infill-frame interaction resulting in shear failure of columns

surrounding frame can further result in localized column shear failure, as shown in Fig. 6. This shear failure can lead to a loss of the axial gravity load carrying capacity of the columns and typically occurs prior to flexural yielding of the columns at low drift levels.

A rigid softening material model is used to incorporate shear degradation in columns. The material model is used in zero-length shear springs, placed in series with the flexural hinges at the end of the columns. Fig. 7 shows the backbone curve for the rigid-softening material model, characterized by initial linear elastic behavior up to the column shear strength (V_n), which is computed by using the model developed by Sezen and Moehle (2004). Shear failure is followed by a negative post-peak slope that captures the shear strength degradation. A high initial stiffness (K_{rigid}) is used for the elastic region, i.e., zero deformation is assumed in the spring up to the shear strength of the column. This assumption is consistent with the fact that column shear failure in infill frames typically occurs at very low drift levels. The deformation parameters for the shear spring are derived from the modeling criteria provided in Tables 6–8 of ASCE/SEI 41 (2007). Elwood et al. (2007) developed a supplement to ASCE/SEI 41 related to existing RC buildings that is based on experimental evidence and empirical models. The supplement includes modeling criteria for columns that have experienced shear failure before flexural yielding. Following the model of Elwood et al. (2007) for column shear failure, axial failure begins after the ultimate shear deformation (δ_u) is reached. In this study, it is conservatively assumed that

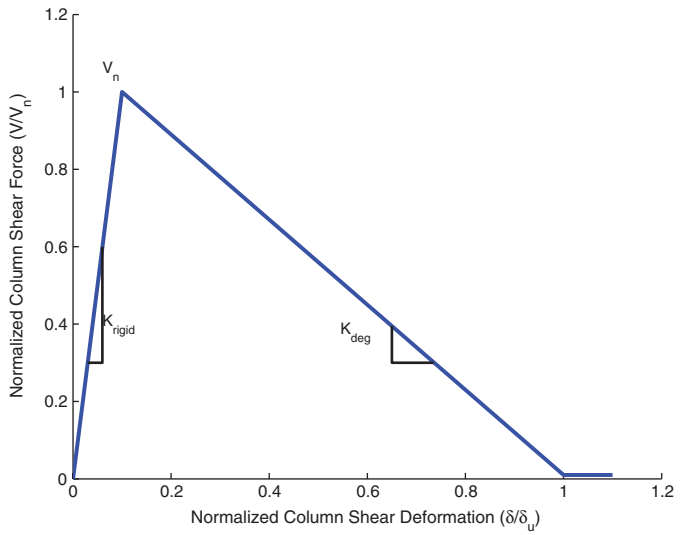

Fig. 7. Backbone curve for shear degrading material model

Table 2. Modeling Parameters for Column Shear Spring

Story	Axial load ratio at shear failure ($P/A_g f'_c$)	Column shear strength, V_n [kips (kN)]	Lateral drift at axial failure (Δ_a/L)
1	0.25	25.2 (112.1)	0.008
2	0.16	25.1 (111.7)	0.010
3	0.07	25.1 (111.7)	0.015

collapse triggered by axial column failure occurs at δ_u. The magnitude of the ultimate shear deformation is influenced by the axial load ratio in the column at the time of shear failure and the shear reinforcing ratio. An iterative approach was employed to determine the axial load ratio at which shear failure occurs. The modeling parameters for the shear spring material model are shown in Table 2.

Overview of Prototype Building and Structural Modeling

The prototype building used for the collapse assessment study is modeled after a design developed previously as part of a multi-university research program on the seismic evaluation and retrofit of nonductile concrete frames with infills. The prototype is a three-story nonductile concrete frame building with unreinforced infills, designed according to engineering practice in California in the 1920s. A plan view of the building and elevation views of the perimeter frames are shown in Fig. 8. The building has three-wythe masonry walls on the perimeter with bare frames on the interior. More details on the structural design of the prototype building can be found in the work of Stavridis (2009).

3D analysis models were developed for the prototype building by using the components described earlier, i.e., beams and columns that incorporate concentrated springs for flexural hinging, shear springs for shear degradation, and pairs of dual compression struts for the infills. The flexural strength used for the column hinges is conservatively based on zero axial load, because preliminary dynamic and pushover analyses showed that the axial demands did not exceed that of the balance point for the column section. This simplifying assumption is supported by parameter studies conducted by Haselton and Deierlein (2007), which showed that the system collapse capacity is much less dependent on the flexural strength, compared to the plastic rotation capacity and cyclic deterioration capacity of the beam and column elements. Further, because the lateral stiffness of the structure is dominated by the infills and the member span to depth ratios are large, the frame is modeled by using centerline dimensions.

The strut model parameters for the infill panels were obtained from the model calibration described earlier. To account for the fact that the test specimens were 2/3-scale, compared to the full scale prototype model, the model parameters were adjusted as follows:

- The ultimate strength was scaled according to the ratio of the infill thickness (t_{inf}) for the 2/3-scale and full-scale specimens;
- The initial stiffness was scaled based on the ratio of ($t_{\text{inf}}/L_{\text{strut}}$) for the 2/3-scale and full-scale specimens, where L_{strut} is the length of the diagonal strut; and
- F_c/F_y, Δ_c/Δ_y, and K_c/K_e were assumed to be the same for the 2/3-scale and full-scale specimens.

Table 3 shows the strut model parameters used in the full-scale building model that were obtained from the calibration exercise discussed earlier and adjusted for scale. The table also shows the strut model parameters obtained from the previous outlined predictive models. The model developed by Mehrabi et al. (1996) was used to compute F_c. K_e was obtained by using the analytical model

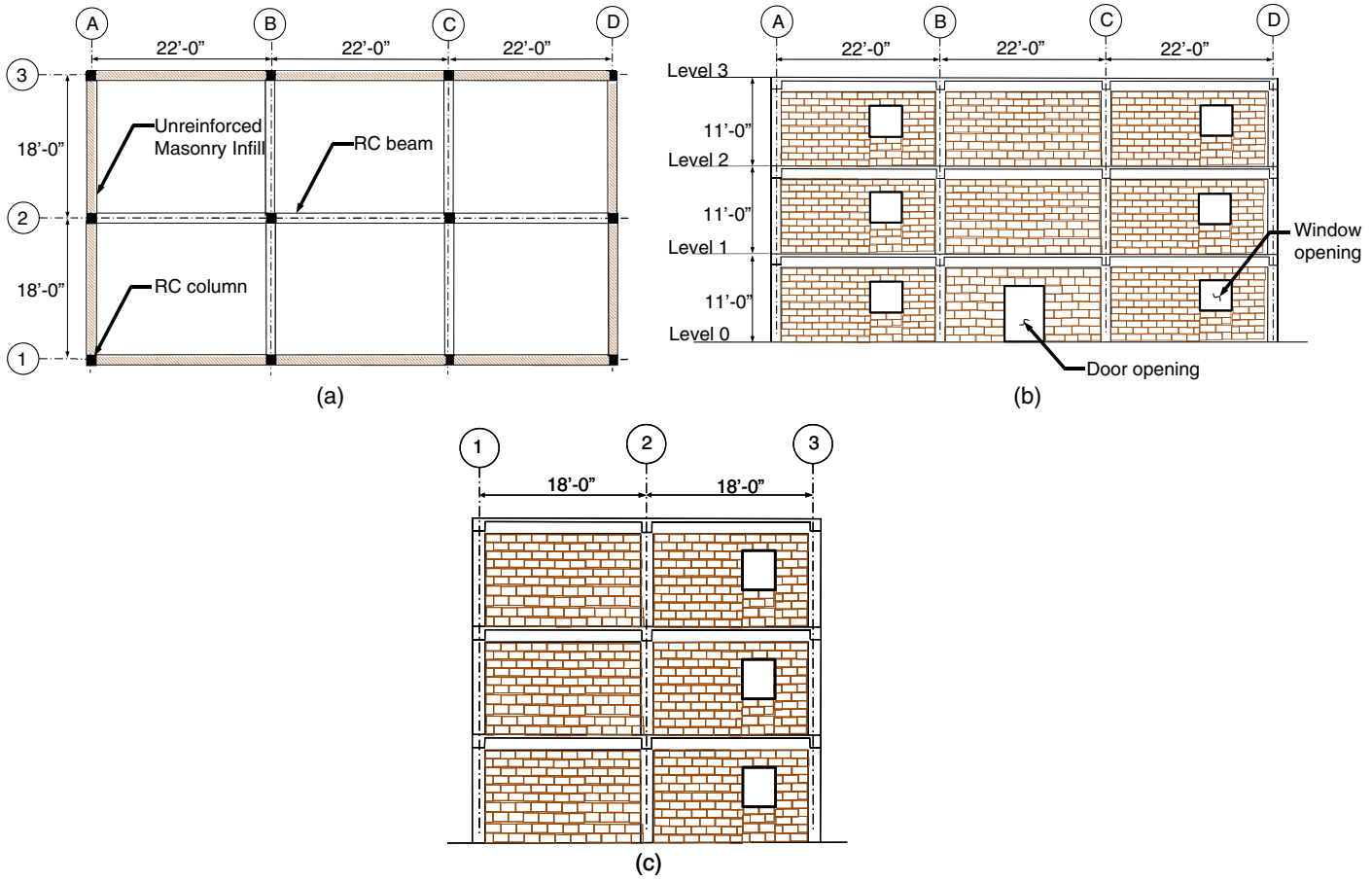

Fig. 8. Prototype building layout: (a) plan view; (b) Line 1 frame elevation; (c) Lines A and D framing elevation [data from Stavridis (2009)]

Table 3. Strut Model Parameters for Full Scale Building Model

	Calibration					Predictive equations/guidelines				
Infilled frame configurations	K_e [kip/in. (kN/mm)]	F_y [kips (kN)]	F_c/F_y	Δ_c/Δ_y	K_e/K_c	K_e [kip/in. (kN/mm)]	F_y [kips (kN)]	F_c/F_y	Δ_c/Δ_y	K_e/K_c
Solid panel	3,984 (697)	195 (867)	1.3	5.2	−0.027	2,144 (375)	180 (800)	1.4	4.5	−0.035
Panel with window opening	1,530 (268)	138 (614)	1.5	7.1	−0.028	1,053 (184)	132 (587)	1.5	6.2	−0.035
Panel with door opening	1,305 (229)	125 (555)	1.7	11.3	−0.032	753 (132)	115 (511)	1.7	9.8	−0.035

provided by Saneinejad and Hobbs (1995). The other parameters (F_c/F_y, Δ_c/Δ_y, K_c/K_e) were used as the mean values from the 14 panel tests described previously.

The concrete floor slab was modeled using a rigid kinematic diaphragm constraint at the floor levels. Foundation uplift was incorporated using compression-only springs at the base of all columns. The force-deformation relationship for the compression-only elastic material is shown in Fig. 9. The compression-only spring was assigned a high compressive stiffness (K_{rigid}) that was large enough to produce negligible compressive deformations (assuming soil deformations to be small), but low enough to avoid numerical problems related to ill-conditioned stiffness matrices. Uplift of the infill frame is partially restrained by the adjacent beams that frame into it at each floor and the foundation level. This partial restraint can lead to tension forces in the columns of the infill frame, even after uplift. The restraint provided by superstructure beams is incorporated into the models used in this study; however, the presence of grade beams is not considered. Additional column tension forces may potentially arise as a result of suction from the soil at the base of the footing; however, these forces are considered to be negligible when compared to the restoring forces generated in the adjacent beams.

As summarized in Table 4, six variants of the 3D building model are developed and used for static and dynamic analyses. The variations are based on the type of deterioration mechanisms and column base supports that are incorporated in each of the models. The variants also include a bare frame model (Case F) and a model developed with strut model parameters based on the guidelines discussed earlier (Case E).

Pushover Results for Prototype Building

Monotonic static pushover analyses are performed on four of the six model variants (Models A, B, C, and D) using the lateral load pattern prescribed in ASCE 7-10 (2010) in both principal directions. Fig. 10 shows the static pushover responses for the four variants with loads applied in the longitudinal direction. Comparison of the pushover responses for Models A and B shows how

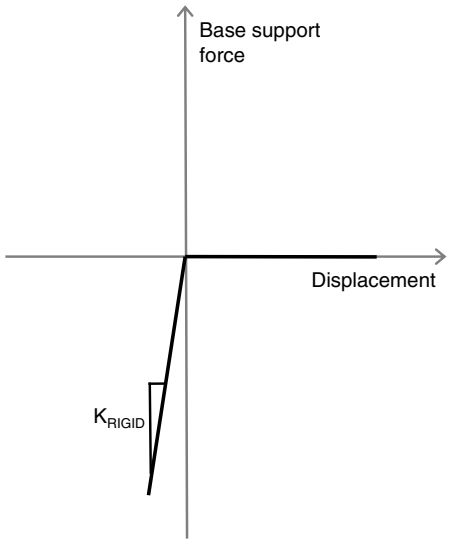

Fig. 9. Schematic of force deformation response for compression-only elastic material used at column base to account for uplift of shallow foundations

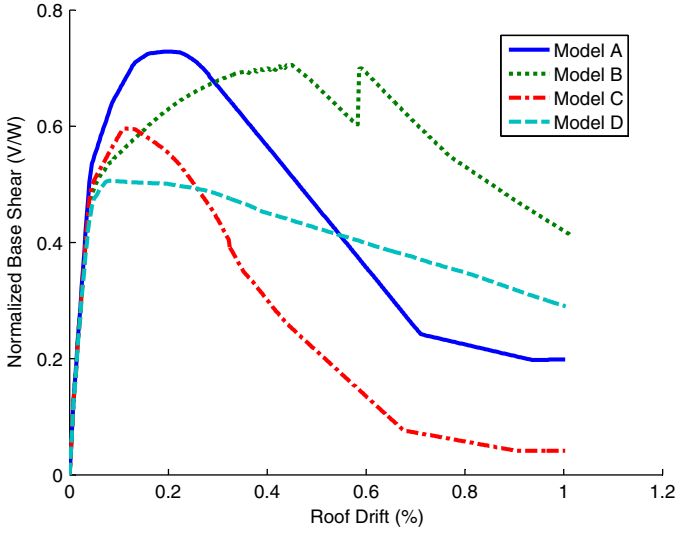

Fig. 10. Monotonic static pushover curve for Models A, B, C, and D for loading in the longitudinal direction

modeling the foundation uplift improves the postpeak ductility. In this case, Model B retains approximately 75% of its lateral strength at 0.8% roof drift compared to Model A, which retains only 30% of its lateral strength at the same roof drift. By chance, the lateral strength of Model B is just slightly less than that of Model A, suggesting that rocking occurs at approximately the same time as the onset of strength degradation in the infill panels. Model C, which includes column shear failure, has a 18% lower ultimate strength than Model A, indicating that omitting column shear failure can be unconservative. The degree of unconservatism obviously depends on the difference in the shear strength between the column and infill. The pushover curve for Model D provides the most representative response, incorporating both foundation uplift and column shear failure. As in the comparison of Models B and A, allowing for column uplift (Model D) increases the system ductility relative to the fixed base case (Model C), although similar to the comparison of Models B and A, the strength of Model D ultimately degrades when the base shear reaches the level associated with column shear failure (V/W equal to approximately 0.51).

Collapse Performance Assessment of Prototype Building

The collapse performance of the six building variants was assessed using the incremental dynamic analyses (IDA) technique. Nonlinear dynamic analyses were run by using the set of 44 far-field ground motion pairs and the scaling method of FEMA P695 (2009). The *OpenSees* structural model is able to simulate most of the significant deterioration modes that contribute to collapse behavior, including axial strength and stiffness deterioration of the infill struts and flexural and shear deterioration of the beam-columns. Axial crushing of columns was indirectly evaluated by using a force-based limit state check, where collapse is assumed to occur when the axial load in any individual column exceeds $A_g f'_c$, where A_g is the gross cross-sectional area of the column and f'_c is the compressive strength of the column concrete. However, this axial force check did not control for any of the building model variants. Another so-called nonsimulated collapse mode that was evaluated is associated with axial column failure following shear failure. For this evaluation, collapse was conservatively assumed to occur when the column shear strength has reduced to zero, corresponding to δ_u based on the backbone curve shown in Fig. 7. This evaluation did control the collapse limit state in several cases.

Fig. 11 shows the collapse IDA plot for Model D for inertial loading in the longitudinal direction. The median collapse capacity occurs at a spectral intensity (Sa_{T1}) of 1.9 g for the longitudinal direction and 1.7 g for the transverse direction. The ground motion record-to-record variation in the collapse capacity had a dispersion (standard deviation of the natural logarithm of the collapse capacity) that ranged from 0.35 to 0.43, which is similar to values reported in other studies of collapse capacity and the default value of 0.4 in FEMA P695 (2009). As shown by the dashed IDA curves in Fig. 11, the nonsimulated column shear-axial failure mechanism

Table 4. Median Collapse Capacity and for All Prototype Model Variants

Model	Infill included	Source of strut model parameters	Column shear deterioration	Footing uplift considered	Median collapse capacity (g)	
					Longitudinal direction	Transverse direction
A	Yes	Calibration	No	No	2.5	2.0
B	Yes	Calibration	No	Yes	2.7	2.3
C	Yes	Calibration	Yes	No	1.8	1.6
D	Yes	Calibration	Yes	Yes	1.9	1.7
E	Yes	Predictive equations	Yes	Yes	1.7	1.5
F	No	N/A	Yes	Yes	1.1	1.5

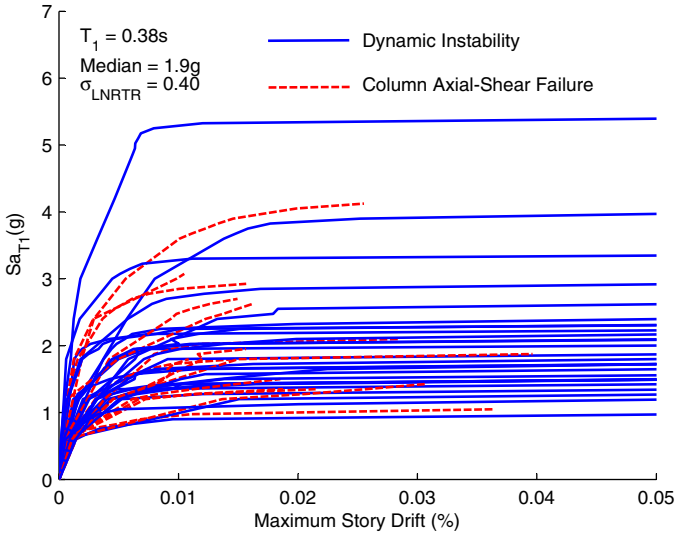

Fig. 11. IDA plot for prototype Model D for loading in the longitudinal direction

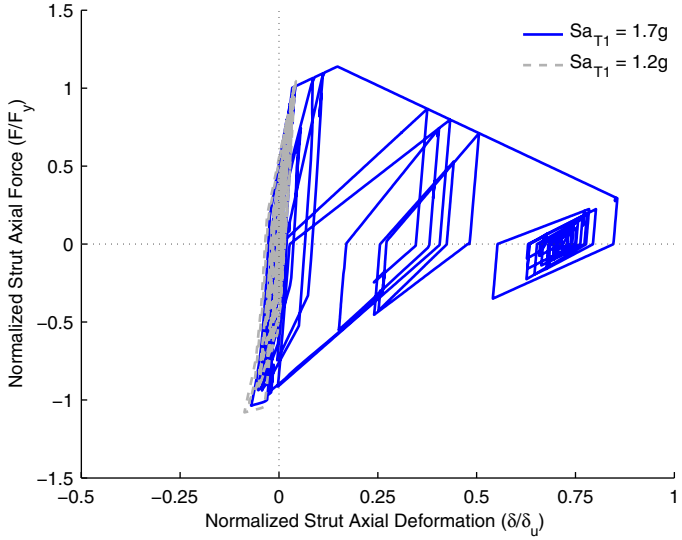

Fig. 12. Hysteretic plots for infill strut model at 1.2 g and 1.7 g spectral intensities

controlled the collapse capacity in approximately 34% of the IDA analyses for loading in the longitudinal direction.

Table 4 summarizes the median collapse capacity for all six building variants in the two principal directions. The results indicate that the median collapse capacity for prototype Model C (with column shear failure) is approximately 12 to 22% less than Model A (without column shear failure), indicating that the exclusion of column shear failure will result in an overprediction of collapse capacity. The level of overprediction for the prototype model variants is consistent with the differences in lateral strength in the pushover response. The median collapse capacity for Model B is 7 to 13% higher than Model A, suggesting that allowance for shallow foundation uplift can improve the collapse performance of infill frames. This improvement in collapse capacity is reduced when column shear failure is incorporated with Model D, whose collapse capacities are 4% higher than those for Model C.

The analysis model based on the predictive strut model parameters (Model E) has a collapse capacity that is 17 to 21% lower than the corresponding model with calibrated parameters (Model D). This difference reflects the differences in model parameters summarized in Table 3. Comparing the two sets of parameters, which are fairly similar except for K_e, seems to suggest that the system collapse capacity is slightly sensitive to the strut stiffness. However, it is reassuring that the collapse capacity determined by the predictive equations is fairly close and slightly conservative compared to the model with the calibrated parameters. More importantly, a comparison of the median collapse capacity of Models D and F shows that the infill panels significantly increase the collapse performance of the prototype building particularly in the longitudinal direction (by a factor of 1.97 in this case). However, this increased capacity provided by the infill is specific to this frame geometry and may not apply to other cases, depending on the height of the building and configuration of the infill panels. The infill panels in this study are regularly laid out both in plan and elevation and are present in all exterior bays, significantly adding to the strength and stiffness of the building. This configuration is quite favorable in comparison to many existing buildings that have irregularly configured infill panels, including weak first-story configurations, where the presence of infill panels may reduce the collapse capacity by concentrating deformations.

Fig. 12 shows hysteretic plots for the pair of diagonal struts used to simulate the solid infill panel located in the first story, between Columns A1 and A2 on column Line A in Model D. The hysteretic plots were extracted for a single ground motion corresponding to Sa_{T1} of 1.2 and 1.7 g, representing "moderate" and "collapse" earthquake intensities for Model D. At the moderate intensity level, the hysteretic plot shows that the strut experiences force demands at the threshold of structural damage. At the collapse intensity level, the infill panel is heavily damaged, experiencing significant strength loss to 30% residual strength. Fig. 13 shows hysteretic plots of the shear spring model in a column that is adjacent to the same infill panel. The plots show that at the moderate intensity level, the column is close to shear failure, but has not yet experienced shear failure. However, at the collapse intensity level, the shear capacity of the column is exceeded, followed by a complete loss of shear strength. These response plots suggest that for this particular ground motion, collapse would be caused by column

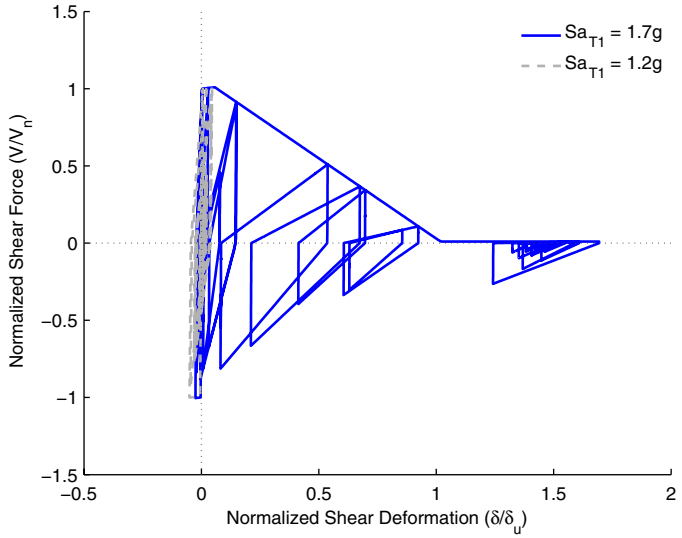

Fig. 13. Hysteretic plots for column shear spring model at 1.2 g and 1.7 g spectral intensities

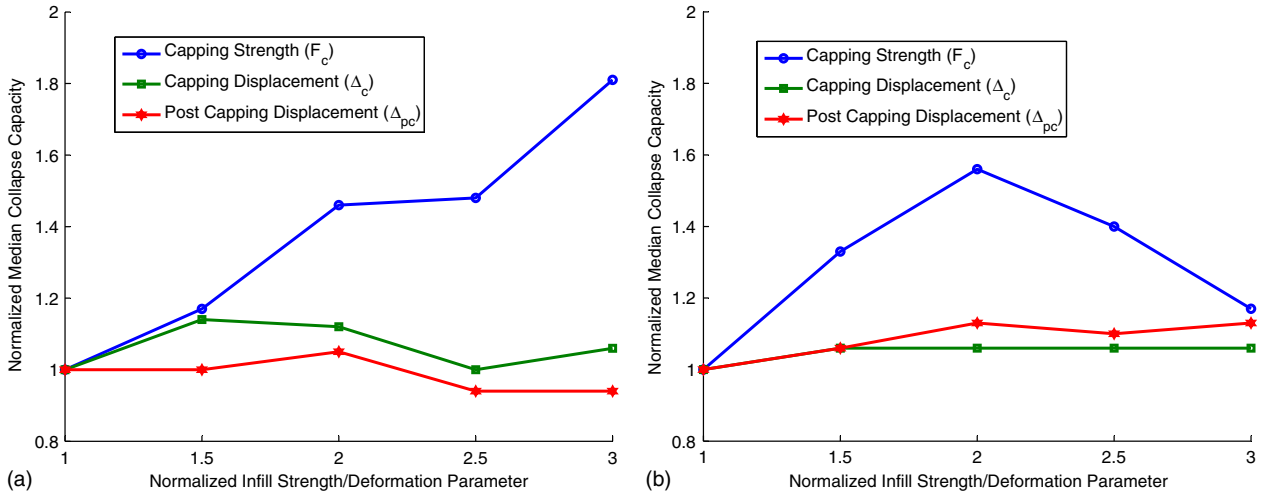

Fig. 14. Effect of strut model strength and deformation parameters on median collapse capacity: (a) Model A; (b) Model C

shear failure, followed by the loss of vertical load carrying capacity of the column.

Effects of Modeling Parameters on Collapse Safety

A two-dimensional (planar) model representing frame Lines A and D (transverse direction) of the prototype building was used to study the impact of the strength and deformation parameters of the infill strut model on collapse performance. Half of the total seismic mass of the building was applied to the two-dimensional model, based on the assumption that the frames with infill panels (Lines A and D in the transverse direction) act as the primary lateral force resisting system. The median collapse capacity for the two-dimensional equivalent of Model D has a spectral intensity of 1.3 g, which is 31% less than its 3D counterpart. This difference is primarily attributed to the contribution of the bare frames to the collapse capacity, which is ignored in the two-dimensional model. Of course, the contribution of bare frames in other infill frame buildings will vary, depending on the relative lateral strength of the frames and infill and the relative number of bare and infill frames.

The sensitivity of the median collapse capacities of the two-dimensional Models A and C to variations in the strength and deformation parameters of the infill are illustrated in Fig. 14. The plots show the median collapse capacity normalized by that of the baseline case versus the normalized strength and deformation parameters. They indicate that the infill strut strength has a significantly larger impact on collapse capacity than the deformation parameters of the strut model. For Models A and C, doubling the infill strength parameter increases the median collapse capacity by 46 and 56% respectively, whereas doubling the infill capping displacement capacity has a negligible impact on the same metric. Fig. 14 also shows that there is a benefit to increasing the infill strength up to a factor of two, however, at higher strengths, there is a reduction in the collapse capacity when column shear deterioration is considered.

Conclusion

This paper summarizes the development and application of analysis tools and guidelines for computing the collapse capacity of nonductile concrete frame buildings with infills. Included is the development of a calibrated infill strut model, in addition to general guidelines for obtaining the model parameters. The study addresses several key questions related to how the collapse capacity is influenced by the effects of infill-column interaction, infill-frame rocking, and column foundation uplift. The IDA technique is applied to several variations of an infill frame building prototype model to examine the effect of these mechanisms on collapse capacity. The results show that incorporating the shear failure of columns, caused by large forces developed in the infill, is critical to the accurate collapse assessment of infill frames, particularly those with nonductile frames. The exclusion of this failure mechanism will lead to unconservative collapse assessments. The extent to which the collapse capacities are overestimated depends on the relative strength of the infill panels and columns. For the building used in this study, incorporating column shear failure leads to a moderate (-12 to -22%) reduction in collapse capacity, compared to analyses in which the column shear failure was not included. Incorporating the effect of uplift or rocking of shallow foundations can have a beneficial influence on the collapse capacity of infill frames. In this study, the allowance for column uplift results in modest ($+7$ to $+13\%$) increases in collapse capacity. However, the results of both the static and dynamic analyses show that the benefits of rocking shallow foundations can be enhanced by avoiding the premature failure of infill panels and surrounding framing members. This study is part of a larger research effort to develop a rocking spine system for infill frames to leverage the beneficial effect of uplifting shallow foundations. The rocking behavior that is induced by the framed-infill spine imposes a uniform deformation mode along the height of the building, thereby reducing the tendency for the formation of a story mechanism.

The strength of the infill dominates the collapse performance of infill frame buildings. However, increasing the infill strength beyond a certain threshold level can have an adverse effect on the collapse performance when infill-column interaction and column shear degradation are incorporated. This result has significant implications to the development of seismic mitigation techniques for infill frames. Care must be taken in implementing new design and retrofit techniques that utilize strong infill panels because this can lead to premature shear failure of the surrounding framing members. The deformation parameters for the infills have a modest impact on collapse capacity, with or without the inclusion of infill-column interaction and column shear degradation. The ASCE/SEI 41 (2007) standard for seismic rehabilitation of existing buildings contains no provisions for considering the effect of shallow foundation uplift in the evaluation of infill frame buildings. The results of this study show that this would result in conservative

assessments, particularly for buildings in which rocking of shallow foundations is expected to occur prior to the failure of infill panels. This suggests that the evaluation procedures of ASCE/SEI 41 (2007) can be improved by incorporating provisions to allow for foundation uplift in infill frame buildings with shallow foundations.

An evaluation of previously proposed analytical models, used to determine infill strut parameters, finds that models considering multiple infill failure mechanisms are more reliable than those that only consider a single mechanism. For the 14 test specimen considered in this study, the strength limit state method proposed by Mehrabi et al. (1996) provided the best estimate of strut strength and the stiffness model proposed by Saneinejad and Hobbs (1995) provided the best estimate of initial strut stiffness. The accuracy of the analytical models can vary significantly based on the predominant failure mechanism in the specimen under consideration. The study demonstrates that strut model parameters obtained by using the proposed guidelines provide a slightly conservative but reasonable estimate of collapse capacity, compared to those obtained from calibration. Evaluation of alternative strut models suggests directions for improving the provisions of the ASCE/SEI 41 (2007) standard for analyzing and evaluating concrete frames with infill walls.

There are several limitations to the collapse assessments presented in this study, which warrant caution in generalizing these results and suggest needs for further research. The influence of out-of-plane failure of infill walls, which may reduce infill resistance and system collapse capacity, was not considered. Shear-axial failure of columns was modeled as a nonsimulated collapse mechanism, whereby axial failure and collapse is conservatively assumed to occur when the shear strength reduces to zero. Although this assumption may be reasonable for lightly reinforced columns, it may be overly conservative for highly confined columns that can maintain their axial strength under large deformations. Finally, the evaluation of the previously developed analytical models for computing the strength and stiffness of infill struts, and the recommendations for obtaining deformation parameters, are based on a limited amount of available test data. A larger pool of available test data would provide a more thorough assessment.

Acknowledgments

Financial support provided to the first author from the Blume Center for Earthquake Engineering, the Engineering Diversity Program and the Diversifying Academia Recruiting Excellence (DARE) Fellowship at Stanford University are gratefully acknowledged. This research is motivated in part by the EERI Framed Infill Network (www.framedinfill.org) initiative and a collaborative project with GeoHazards International. The authors also acknowledge valuable discussions on the research with K. Mosalam, D. Mar, J. Rogers, and S. Billington.

References

ASCE. (2007). "Seismic rehabilitation of existing buildings." *ASCE/Structural Engineering Institute (SEI) 41*, Reston, VA.

ASCE. (2010). "Minimum design loads for buildings and other structures." *ASCE 7-10*, Reston, VA.

Asteris, P. (2003). "Lateral stiffness of brick masonry infilled plane frames." *J. Struct. Eng.*, 10.1061/(ASCE)0733-9445(2003)129:8(1071), 1071–1079.

Blackard, B., William, K., and Mettupulayam, S. (2009). "Experimental observations of masonry infilled reinforced concrete frames with openings." *Special Publication SP-265*, American Concrete Institute, Farmington Hills, MI.

Chrysostomou, C. (1991). "Effects of degrading infill walls on the nonlinear seismic response of two-dimensional steel frames." Ph.D. dissertation, Dept. of Civil and Environmental Engineering, Cornell Univ., Ithaca, NY.

Colangelo, F. (2005). "Pseudo-dynamic seismic response of reinforced concrete frames infilled with non-structural brick masonry." *Earthquake Eng. Struct. Dyn.*, 34(10), 1219–1241.

Dolsek, M., and Fajfar, P. (2008). "The effect of masonry infills on the seismic response of a four-story reinforced concrete frame—A deterministic assessment." *Eng. Struct.*, 30(7), 1991–2001.

Elwood, K., et al. (2007). "Update to ASCE/SEI 41 concrete provisions." *Earthquake Spectra*, 23(3), 493–523.

FEMA. (2009). "Quantification of building seismic performance factors." *FEMA P695*, Applied Technology Council, Redwood City, CA.

Giannakas, A., Patronis, D., and Fardis, M. (1987). "The influence of the position and the size of openings to the elastic rigidity of infill walls." *Proc., 8th Hellenic Concrete Conf.*, Hellenic Concrete Society, 49–56.

Haselton, C., and Deierlein, G. (2007). "Assessing seismic collapse safety of modern reinforced concrete frame buildings." Ph.D. dissertation, Dept. of Civil and Environmental Engineering, Stanford Univ., Stanford, CA.

Haselton, C. B., Liel, A. B., Lange, S. L., and Deierlein, G. (2008). "Beam-column element model calibrated for predicting flexural response leading to global collapse of RC frame buildings." Pacific Earthquake Engineering Research Center, Berkeley, CA.

Ibarra, L. F., Medina, R. A., and Krawinkler, H. (2005). "Hysteretic models that incorporate strength and stiffness deterioration." *Earthquake Eng. Struct. Dyn.*, 34(12), 1489–1511.

Kyriakides, M. (2011). "Seismic retrofit of unreinforced masonry infills in non-ductile reinforced concrete frames using engineered cementitous composites." Ph.D. dissertation, Dept. of Civil and Environmental Engineering, Stanford Univ., Stanford, CA.

Lignos, D. G., and Krawinkler, H. (2013). "Development and utilization of structural component databases for performance-based earthquake engineering." *J. Struct. Eng.*, 10.1061/(ASCE)ST.1943-541X.0000646, 1382–1394.

Mehrabi, A. B., Shing, P. B., Schuller, M., and Noland, J. (1996). "Performance of masonry-infilled reinforced concrete frames under in-plane lateral loads." *Rep. CU/SR-94/6*, Dept. of Civil, Environmental and Architectural Engineering, Univ. of Colorado at Boulder, Boulder, CO.

Mondal, G., and Jain, K. (2008). "Lateral stiffness of masonry infilled reinforced concrete frames with central opening." *Earthquake Spectra*, 24(3), 701–723.

Open System for Earthquake Engineering Simulation (OpenSees) [Computer software]. Pacific Earthquake Engineering Research Center, Univ. of California, Berkeley.

Saneinejad, A., and Hobbs, B. (1995). "Inelastic design of infilled frames." *J. Struct. Eng.*, 10.1061/(ASCE)0733-9445(1995)121:4(634), 634–650.

Sattar, S., and Liel, A. (2010). "Seismic performance of concrete frame structures with and without masonry infill walls." *9th US National and 10th Canadian Conf. on Earthquake Engineering*, Earthquake Engineering Research Institute, Oakland, CA.

Sezen, H., and Moehle, J. (2004). "Shear strength model for lightly reinforced concrete columns." *J. Struct. Eng.*, 10.1061/(ASCE)0733-9445(2004)130:11(1692), 1692–1703.

Stafford-Smith, B., and Carter, C. (1969). "A method for the analysis of infilled frames." *Proc. Inst. Civ. Eng.*, 44(1), 31–48.

Stavridis, A. (2009). "Analytical and experimental study of seismic performance of reinforced concrete frames infilled with masonry walls." Ph.D. dissertation, Dept. of Structural Engineering, Univ. of California, San Diego.